



This is a repository copy of *Impact of blade structural and aerodynamic uncertainties on wind turbine loads*.

White Rose Research Online URL for this paper:  
<https://eprints.whiterose.ac.uk/183343/>

Version: Published Version

---

**Article:**

Gonzaga, P., Toft, H., Worden, K. et al. (4 more authors) (2022) Impact of blade structural and aerodynamic uncertainties on wind turbine loads. *Wind Energy*. ISSN 1095-4244

<https://doi.org/10.1002/we.2715>

---

**Reuse**

This article is distributed under the terms of the Creative Commons Attribution (CC BY) licence. This licence allows you to distribute, remix, tweak, and build upon the work, even commercially, as long as you credit the authors for the original work. More information and the full terms of the licence here:

<https://creativecommons.org/licenses/>

**Takedown**

If you consider content in White Rose Research Online to be in breach of UK law, please notify us by emailing [eprints@whiterose.ac.uk](mailto:eprints@whiterose.ac.uk) including the URL of the record and the reason for the withdrawal request.




[eprints@whiterose.ac.uk](mailto:eprints@whiterose.ac.uk)  
<https://eprints.whiterose.ac.uk/>

## RESEARCH ARTICLE

WILEY

# Impact of blade structural and aerodynamic uncertainties on wind turbine loads

Paulo Gonzaga<sup>1,2</sup>  | Henrik Toft<sup>1</sup> | Keith Worden<sup>2</sup> | Nikolaos Dervilis<sup>2</sup> | Lars Bernhammer<sup>1</sup> | Nevena Stevanovic<sup>1</sup> | Alejandro Gonzales<sup>1</sup>

<sup>1</sup>Loads and control, Siemens Gamesa Renewable Energy, Brande, Denmark

<sup>2</sup>Department of Mechanical Engineering: Dynamics Research Group, The University of Sheffield, Sheffield, UK

## Correspondence

Paulo Gonzaga, Borupvej 16, Brande, 7330, Denmark.

Email: phgonzaga1@sheffield.ac.uk

## Abstract

Offshore wind power has been in the spotlight among renewable energy sources. The current trends of increased power ratings and longer blades come together with the aim to reduce energy costs by design optimisation. The standard approach to deal with uncertainties in wind-turbine design has been by the use of characteristic values and safety factors. This paper focusses on modelling the effect of structural and aerodynamic uncertainties in blades. First, the uncertainties in laminate properties are characterised and propagated in a blade structural model by means of a Monte Carlo simulation. Wind tunnel measurement data are then used to define the variability in lift and drag coefficients for both clean and rough aerofoil behaviour, which is then used to extrapolate rough behaviours throughout the blade. A stochastic spatial interpolation parameter is used to define the evolution of the degradation level. The combined effect and the variance contribution of these two uncertainty sources in turbine loads is finally defined by aeroelastic turbine simulation. This research aims to provide a framework to deal with uncertainties in wind-turbine blade design and understand their effects in turbine behaviour.

## KEYWORDS

aeroelastic simulation, probabilistic design, sensitivity analysis, uncertainty quantification, wind turbine blade

## 1 | INTRODUCTION

Offshore wind farms are expected to continue being one of the leading forces, both in the transition to renewable energy and in the economic domain. There have been continuous efforts to mature technology, reduce costs and make offshore wind more competitive with traditional energy sources. Even though much has been accomplished, there are still opportunities to improve.

Uncertainties are omnipresent in the wind industry, both in the external conditions (such as wind and waves), as well as in the structures' properties (tower and blade) and in models that are used to predict key quantities such as costs, energy yield and structural loads.<sup>1</sup> Some of the phenomena involved in generating power from wind (anisotropic materials, aeroelasticity, control, wind forecasting, sea waves, wind-farm wakes) can still be too complex for current prediction capabilities.

The growing attention in wind-energy applications to the importance of defining the uncertainty effect on predictions is in parallel with the urge for design optimisation and lowering of energy costs. Predictions are the result of a combination of measurements, modelling and

-----  
This is an open access article under the terms of the Creative Commons Attribution License, which permits use, distribution and reproduction in any medium, provided the original work is properly cited.

© 2022 The Authors. *Wind Energy* published by John Wiley & Sons Ltd.

simulations. A standard assumption is that reality will not move significantly away from these predictions; meaning that small perturbations of the system will only cause small perturbations of the predictions.<sup>2</sup> However, only within a probabilistic framework can such assumptions be deemed reasonable.

Before an expensive wind farm is constructed in the uncertain and rapidly-varying environment of the rough sea, its construction, design and maintenance are thoroughly assessed to determine (and under a given set of constraints maximise) the energy output and the lifetime of the wind turbines. The procedures to determine the energy output and life time of a wind farm are fixed in the IEC standard.<sup>3-6</sup>

Structural design and analysis have initially been based on deterministic models. However, it is potentially advantageous that probabilistic-based methods could be employed, because of the uncertainties in loads, strengths, and structural modelling. As a fundamental design requirement, a structure is expected to perform satisfactorily within its full design life. This condition means that wind turbines must fulfil specific functional requirements and do not become unsafe over, generally, at least 20 years.<sup>3</sup>

Frequently, only a limited number of uncertain parameters can be taken into account in such studies<sup>7-9</sup> and the structural and aerodynamic uncertainties' combined effect is not often considered or a trustworthy uncertain characterisation is not available. The eventual deviations are expected to be covered by the partial safety factors defined by the IEC standard.<sup>3</sup>

To address the challenge of providing a reality-bounded uncertainty characterisation and to evaluate the effect of combined structural and aerofoil roughness uncertainties, this study aims to (a) develop a framework to propagate and validate uncertainties in laminate properties with blade full-scale testing; (b) utilise wind-tunnel test data to define rough behaviour for different aerofoils throughout the blade; (c) compare uncertainty levels to IEC61400-5<sup>4</sup> recommended tolerances for blade design; and (d) predict the effect of these uncertainties in wind turbine loads and energy production using aeroelastic simulation.

The performance of wind turbine aerofoils—measured in terms of the aerodynamic coefficients of lift, drag and moment—is considered to be an important source of uncertainty in wind turbine simulation. During operation, the surface of a blade can be contaminated by dust, dirt, insects and so on. The changes in surface roughness during operation may result in significant uncertainties in power capture and loading.<sup>10</sup>

Surface roughness is a common feature of most operating aerofoil surfaces; it may arise from the manufacturing process, period of service, insect contamination and/or natural accumulation from weather-related events.<sup>11</sup> In wind turbine blades, excessive surface roughness can force laminar-turbulent transition in the boundary layer to happen much sooner than on a clean aerofoil, which can result in increased drag, lower lift and therefore less energy captured. The rough behaviour of an aerofoil is frequently investigated in wind tunnel experiments by means of zigzag-tape<sup>12</sup> (or tripwire) application, which triggers the transition. In this way, for any given section along the span of a blade, the designer can choose to use clean, rough or moderate roughness aerofoil characteristics.<sup>13</sup> Special attention has been given to investigate the effect of uncertainties on the aerodynamic behaviour of blades. Another important factor contributing to these uncertainties is lead-edge erosion,<sup>14</sup> which is acknowledged to cause a major reduction in energy production of a wind turbine.

This paper is organised as follows: Section 2 presents the propagation of laminate uncertainties on a blade structural model and the validation of the results via a full-scale blade static deflection test. Model and experimental results for blade mass and CG (centre of gravity) location are also compared. Section 3 presents the stochastic model for the blade aerodynamic coefficients, using wind tunnel test data to define rough aerofoil conditions and a interpolation scheme between clean and rough conditions that varies along the blade span. Section 4 discusses the methodology adopted in the present study, which uses Monte Carlo simulations on a turbine aeroelastic model to propagate and evaluate the uncertainty effect on wind turbine loads and finally, Section 5 presents the conclusions drawn from the present study.

## 2 | STRUCTURAL UNCERTAINTIES

This sections describes the procedure to characterise and propagate the uncertainty of laminate material properties on a blade structural model by means of a Monte Carlo simulation. The validation of the results is achieved by comparison with data from a full-scale wind turbine blade static test.

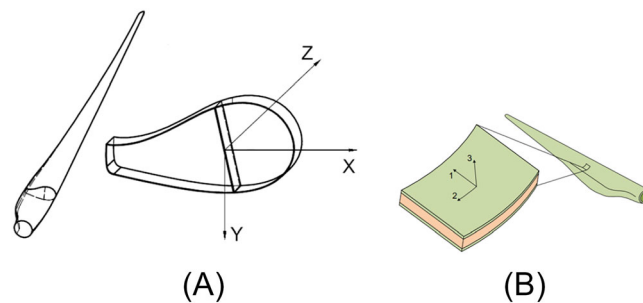
### 2.1 | Uncertainties characterisation

Laminate material properties are subjected to random uncertainty during production. There can be many factors altering the standard behaviour expected from a glass-fibre composite.

The material stiffness and strength for the glass-fibre laminates are determined from material testing of actual fibre-resin and core materials that are representative of the blade production laminates and sandwich configurations. Testing for each material property was carried out according to the relevant standards.<sup>15</sup> The experimental information available: the number of tests and coefficient of variation (Equation (1)) for each property, is presented at Table 1.  $E_{ij}$  is the modulus of elasticity in the direction  $i$ ,  $G_{ij}$  the shear modulus of elasticity in the  $ij$  direction,  $\rho$  the laminate density and  $t$  the laminate thickness. The coefficient of variation is defined by,

**TABLE 1** Material properties experimental CoV

Property	CoV %	# test	Distribution	Property	CoV %	# tests	Distribution
BIAX							
$E_{11}$	4	15	Normal	$G_{12}$	3	30	Normal
$E_{22}$	4	15	Normal	$G_{13}$	3	5	Normal
$E_{33}$	4	15	Normal	$G_{23}$	3	5	Normal
$\rho$	0.6	27	Normal	$t$	2	27	Normal
UD							
$E_{11}$	3	15	Normal	$G_{12}$	3	15	Normal
$E_{22}$	5	15	Normal	$G_{13}$	3	15	Normal
$E_{33}$	5	15	Normal	$G_{23}$	3	15	Normal
$\rho$	0.6	9	Normal	$t$	3	9	Normal

**FIGURE 1** (A) Reference system for wind turbine blade; (B) reference for material properties

$$\text{CoV} = \frac{s}{\bar{x}} \cdot 100\% \quad (1)$$

where  $s$  is the standard deviation and  $\bar{x}$  the mean value (for a sample). The uncertain inputs considered in this analysis are the material properties of the two main types of glass-fibre reinforcements used in the blades:

- UD: Unidirectional glass fibre laminate,
- BIAx: Bi-directional glass fibre laminate.

For each type of fibre, the main material properties were considered as random input parameters. CoV data from material testing and nominal values were used to fit probability density functions (PDFs) to these inputs. Normal distributions were used for all variables because, with a normal distribution, the differential entropy is maximised for a given variance,<sup>16</sup> which means it is the least-assuming distribution one can use when having access to only standard deviation and mean values. Even though the normal distribution can achieve negative values (which is not physically possible for material properties) the probability of the negative region is below  $10^{-8}$  for the moduli, and below  $10^{-5}$  for the density and thickness; this means that for any practical sampling implementation (which will be discussed later) the simplified approach using normal distribution is justified and sufficient. The normalised parameters for the distributions (with mean values  $\mu = 1$ ) are presented in Table 1.

## 2.2 | Blade structural model

The cross-sectional model used in this study is based on the formulations of Krenk and Jeppesen<sup>17</sup>; utilising a line mesh in the calculation of the structural features, the torsion and shear properties of the cross-sections are formulated within a finite element method (FEM) with the warping function as unknown. The cross section is divided into straight elements with uniform trapezoidal thickness. Every component is simplified and lumped into a thin-walled shell structure with the help of so-called 'superelements'. The cross-sectional model also calculates the sectional mass by summing the contribution of each layer of the laminate. The main inputs include: geometry, material layup and material properties. The outputs of this model can be listed: blade stiffness distribution in flapwise, edgewise and torsional direction, mass and moment of inertia distribution.

The quantities of interest (QoIs) for this study are: the distributions of stiffness in the flapwise ( $EI_x$ ), edgewise ( $EI_y$ ) and torsional ( $GI_z$ ) directions, as well as blade mass and CG location; these are based on the blade reference frame shown in Figure 1A, where  $z$  direction is perpendicular to the root plane of the blade, and  $x$  and  $y$  are aligned with the pitch coordinate system. Elastic moduli are termed in accordance with a material coordinate system seen in Figure 1B, where the one direction corresponds to the  $0^\circ$  fibre direction.

The calculation is repeated for each cross section throughout the blade (Figure 1A), along the blade span. Deterministic stiffness distributions can be seen in Figure 2A, normalised by their maximum value.

The blade layup is important information because, as can be seen in Figure 2B, there are substantial differences of composition along the blade span; this will show that the type and quantity of laminate used for specific regions of the blade have different impacts on its responses.

### 2.3 | Uncertainty propagation

The Monte Carlo Method (MC) is a widespread methodology for uncertainty propagation because of its non-intrusiveness to the deterministic model, as it can be applied with little to no alteration of previously implemented deterministic code. It consists of building a set of realisations of a model based on its random input characteristics, and then using the collection of these realisations to compute relevant statistics of the model outputs. The estimates converge inevitably to the real probabilities, as a consequence of the law of large numbers (as long as the number of samples is *large* enough and the random input characterisation is correct).

Latin Hypercube Sampling (LHS) is widely used in Monte Carlo simulations as a way to improve accuracy and lower computational cost. LHS is a method to generate controlled random samples; the idea is to take the sampling point distribution close to the probability density function. It

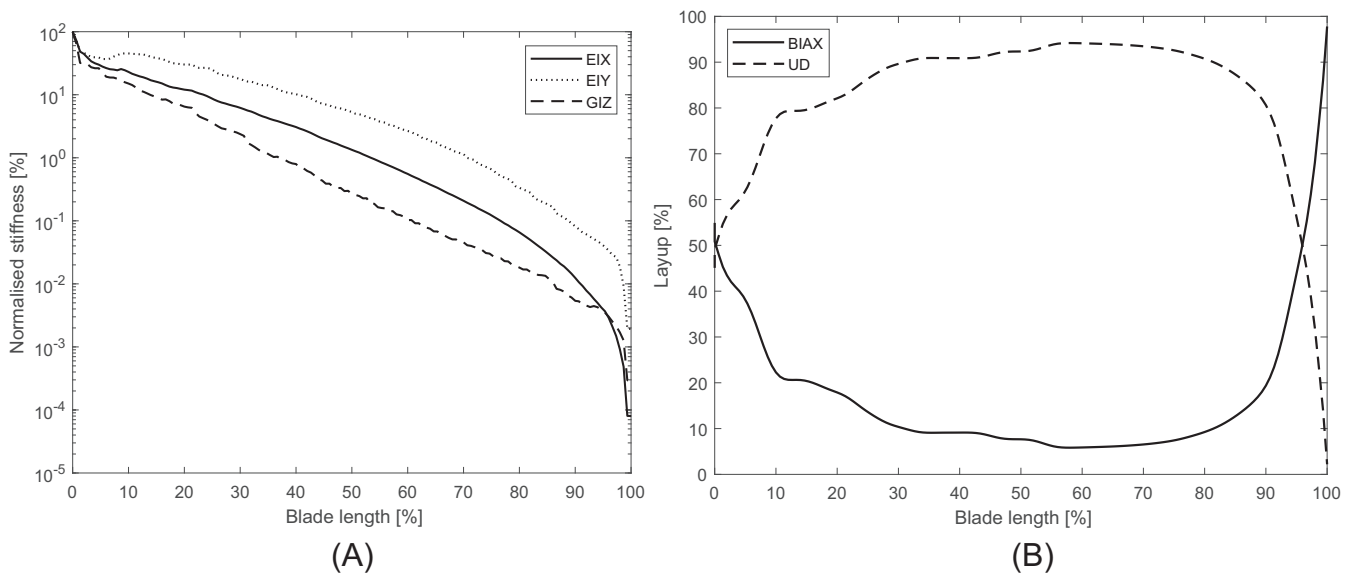


FIGURE 2 (A) Deterministic stiffness distributions; (B) blade layup

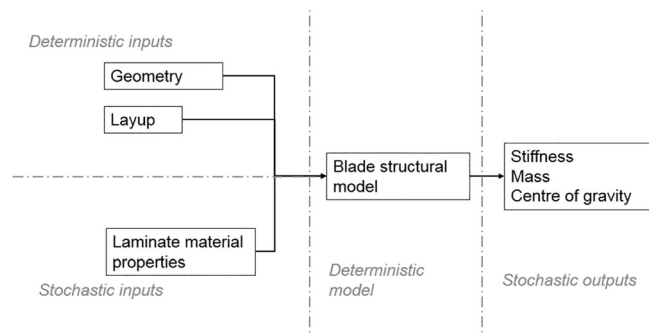
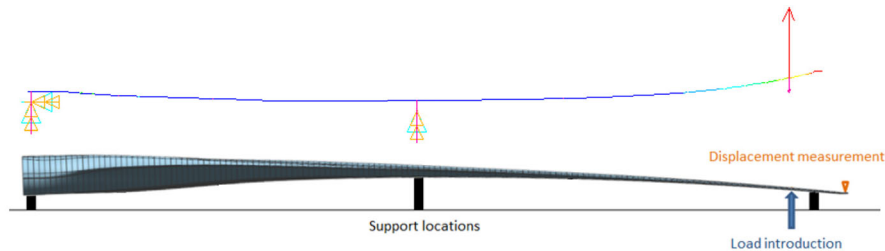


FIGURE 3 Uncertainty propagation on wind turbine blade model

**TABLE 2** Uncertainty levels for blade mean structural parameters

Parameter	Distribution	CoV (%)
Mass moment	Normal	1.2
Mean flapwise stiffness	Normal	2.8
Mean edgewise stiffness	Normal	3.5
Mean torsional stiffness	Normal	2.7

**FIGURE 4** Wind turbine blade static test: finite element model

involves dividing the cumulative density function (CDF) into  $n$  equal partitions and then sampling a specified number of random data points in each partition. An LHS sampling was used to define 5000 samples of the laminate material properties and the collocation of realisations used to describe the effect of the uncertainty on the blade structure. The uncertainty propagation scheme can be seen in Figure 3. This study relies on the following assumptions:

- no correlation between random variables (i.e., all properties were considered to be independent);
- no uncertainties in the external geometry of the blade were considered;
- no uncertainties in the layup of the blade were considered;
- the CG and mass were assumed to be dependent exclusively on the density and thickness of the laminate.

It is customary to present the mean stiffness values as a characteristic for the blade. Another common quantity is the mass moment (defined as the moment caused by the blade weight around its root section). Table 2 presents the coefficient of variation for the Monte Carlo Latin Hypercube Sampling simulation results (MC-LHS) for the mean (over the span-wise direction) blade stiffness and mass moment.

The most critical stiffness is in the flapwise direction; the results show a CoV of 2.8%, which is close to the CoV of the UD  $E_{11}$  (main laminate used on the blade span). This effect can be interpreted as a linear propagation from the material property to blade stiffness. ‘Flapwise’ is the direction where the biggest blade deflection takes place during turbine operation (and it is also a design driver in modern blades). The effect on mass moment is also of interest; for big rotors, it tends to directly impact the dimensioning of the bearing size and there is also a special concern about mass imbalance, which can lower turbine performance and decrease the lifetime of components (e.g., bearings).

## 2.4 | Uncertainty validation

In order to validate the results presented in Table 2, a measure of blade stiffness is necessary. Full-scale blade tests are executed to fulfil both standards/certification requirements and production quality control. One of the parameters assessed in such tests is the blade stiffness (by means of the blade deflection). By propagating the results of the stochastic model of the blade structure in a simulation of such a test and comparing with the experimental data, one can determine whether the model is appropriate.

The blade static deflection test described in this section is a test whose goal is to check the blade structural soundness and give evidence that the blade is neither too stiff nor too flexible. The test setup consists of the blade supported at the root section and at midspan subjected to a negative flapwise load close to the tip. The blade is essentially kept in rigid-body statics due to its own weight pushing it on the supports. This test is not to be mistaken with the full-scale blade test for verification of extreme loads.

Data from a static deflection test of the same type of blade whose structure uncertainty was previously defined, which were all subjected to the same load, will be compared with uncertainty propagation results for the test simulation model. The experimental data consist of 95 blades measured for CG location and blade mass, and 34 blade static-deflection tests.

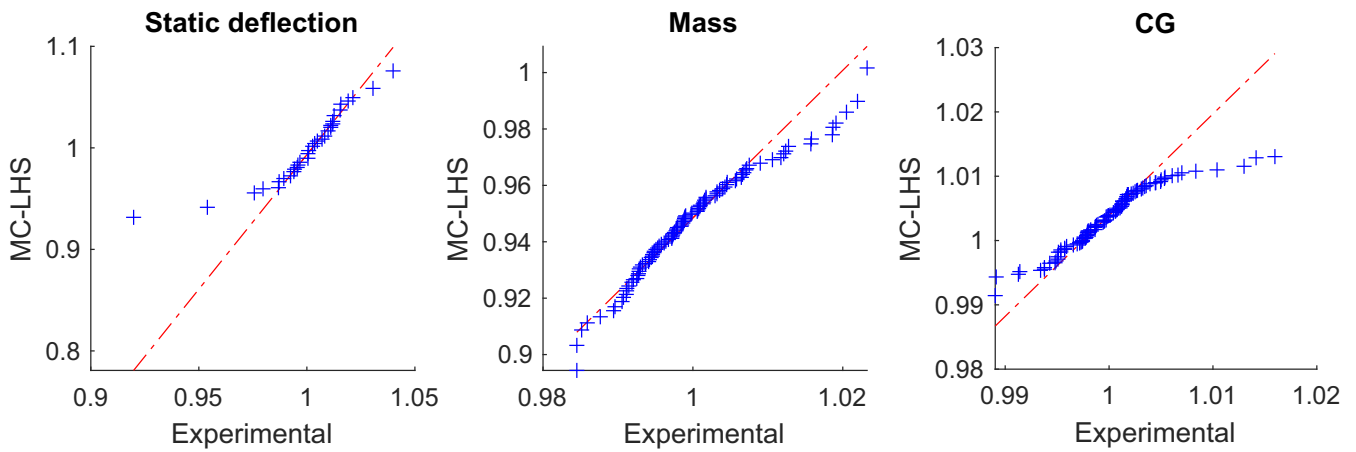


**FIGURE 5** QQ-plot simulation Monte Carlo Method Latin Hypercube Sampling (MC-LHS) versus experimental results

**TABLE 3** Uncertainty levels comparison between simulation and experiment

Parameter	CoV (%)		Mean value	
	Experimental	MC-LHS	Experimental	MC-LHS
Mass	0.90	1.00	1.00	1.00
CG	0.60	0.50	1.00	1.00
Mass moment	1.10	1.10	1.00	1.00
Static deflection	2.20	3.50	1.00	1.00

The setup is illustrated by a 3D model in Figure 4. To simulate this test, a nonlinear beam model is based on the lengthwise stiffness distribution of the blade (which is characterised by the cross-sectional model).

A Monte Carlo study (MC-LHS) for the nonlinear beam model was performed to study the propagation of the material property uncertainty in the blade static-deflection test. The loading force is considered to be deterministic and the blade stiffness distribution realisations from the previous section were used as random inputs.

Both the experimental data and the simulation (MC-LHS) results were normalised in relation to the mean experimental value. Quantile-quantile plots (qq-plot) for experimental versus MC-LHS results can be seen in Figure 5. These data can be used to justify the assumption that both experimental and simulation results from the MC-LHS come from the same normal distribution, even though the qq-plot indicates a limited 'heavy tail' behaviour. The statistical moments for the fitted PDF are presented in Table 3.

A few observations can be made:

- The MC-LHS has virtually the same expected value as the experimental data; this can be interpreted as a well-calibrated, accurate deterministic model for both the blade structural properties and the test simulation (for the deterministic simulation, where the nominal material properties are used as inputs in the blade model, the difference between the simulated static deflection and the mean value of the experiments is lower than 1%).
- The CoVs for both mass and CG differ little from experimental CoVs, which can be interpreted as an accurate representation for the density and laminate thickness uncertainties (which are the only ones affecting CG and mass, and also have the lowest CoVs, Table 1).
- The simulated CoV for the static deflection is higher than the variations seen in the experimental data; this suggests that the variations in laminate stiffness that actually happen in the blades are smaller than the variations seen on coupon-testing data. Another possibility is that the independent characterisation of laminate properties is too pessimistic. In reality, it could be expected that there are correlations between different stiffness terms and mass. However, the lack of experimental evidence to define this correlation model justifies the independence assumed as a conservative approach;
- The CoV of E11 of the UD fibre (3%), which is the main fibre property in the direction of the blade span, can be seen almost directly propagating to the mean flapwise stiffness (CoV = 2.8%) and to the static deflection (CoV = 3.5%). This observation is in accordance with the idea that there are no nonlinear effects happening in the blade static deflection and uncertainties in material properties should be seen directly in the deflection. Nevertheless is also relevant to highlight the fact that the number of experimental data is insufficient to characterise the tails of the

distribution, but as seen in Figure 5A there are at least two points in the lower tail of the experimental data that are outside of the expected linear, normally distributed propagation.

The design and load predictions on blades have had a continuous development with the evolution of high-fidelity models. Wind turbine blades became more flexible and their design more dependent on advanced physical description and require better understanding of deviations from the nominal behaviour. To determine the effect of the laminate properties uncertainties in the blade structure and validate this description with full-scale blade test is the first step to build a framework to understand the impact on wind turbine loads. The next section will focus on defining the blade aerodynamic uncertainties before studying these at turbine level.

### 3 | AERODYNAMIC UNCERTAINTIES

The uncertainty in aerodynamic characteristics is a frequent research topic within wind energy and has been studied in previous works,<sup>10,18–21</sup> among others. Many factors contribute to the uncertainty in aerodynamic properties of wind turbine blade aerofoils (e.g., surface roughness, 3D effect, geometry, stall behaviour, wind tunnel measurements and shape distortion). Because lift and drag coefficients are used as inputs in the aeroelastic simulations to predict turbine loads and annual energy production (AEP), there is an extensive effort to define these values as accurately as possible.<sup>13</sup> The assessment of aerodynamic properties in wind turbine blades and their uncertainty is obtained by a combination of experimental and numerical techniques, normally involving CFD (computational fluid dynamics) simulations and wind tunnel measurements. However, this is usually performed only to characterise the ‘clean state’ of a blade; even though the effects of blade contamination can be seen in turbine outputs, its simulation and validation is seldom possible. The clean state of an aerofoil means its nominal aerodynamic behaviour, without any contamination or geometric deviation; this is the state typically considered in wind turbine simulations and in most wind-tunnel experiments. Surface roughness is a common feature of most operating aerofoil surfaces; it may arise from the manufacturing process, period of service, insect contamination, and/or natural accumulation from weather-related events.<sup>11</sup> In wind turbine blades, excessive surface roughness can cause transition in the boundary layer, which can result in increased drag, lower lift and therefore less energy captured. The rough behaviour of an aerofoil is frequently investigated in wind tunnel experiments by means of zigzag-tape<sup>12</sup> (or tripwire) application, which trigger the transition.

In this section, the focus is to define a stochastic model for the aerodynamic properties of a wind turbine blade based on geometric tolerances, wind tunnel measurements and surface roughness. These uncertainties are driven by physical uncertainty (aleatory) or simply driven by lack of evidence (measurement or model uncertainty) as shown in Table 4. The results will be presented in terms of a design-specific lift coefficient,  $CL_D$ , which happens at  $AoA_D$ , the design specific angle of attack. These are particular to each of the aerofoils discussed throughout this section.

#### 3.1 | Geometric tolerances

A wind turbine blade is built with a complex geometric evolution; it starts with a cylindrical aerofoil, with  $RT = 100\%$  (relative thickness) that evolves to a thinner profile towards the tip (that can be as low as  $RT = 15\%$ ). Geometric uncertainties can come from any distortions of the blade aerofoils during manufacturing, handling, transportation or installation. Because static aerodynamic coefficients are defined based on a nominal geometry, it is important to evaluate the effects on aerodynamic coefficients resulting from geometric distortion. IEC 61400-5:2020<sup>4</sup> defines functional design tolerances that must be accounted for in the evaluation of loads, performance and structural integrity. The tolerance for aerofoil local chord length is set at  $\pm 1\%$ .

Without 3D scanning or detailed measurement of a blade's geometry, the impact of (a worst-case scenario based on the IEC tolerance for) geometric distortions on lift coefficient (CL) can be quantified in a Monte Carlo simulation. The aerodynamic coefficients of a distorted aerofoil ( $RT = 18\%$ ) are computed in XFOIL.<sup>22</sup> The chord length of the aerofoil is considered to be a uniform random variable with bounds defined at  $\pm 1\%$

**TABLE 4** Sources of uncertainty included in this study

	Physical	Measurement
Geometric tolerance	x	
Surface roughness	x	
Variation in wind tunnel measurement: clean		x
Variation in wind tunnel measurement: rough		x
Degradation level throughout the blade	x	



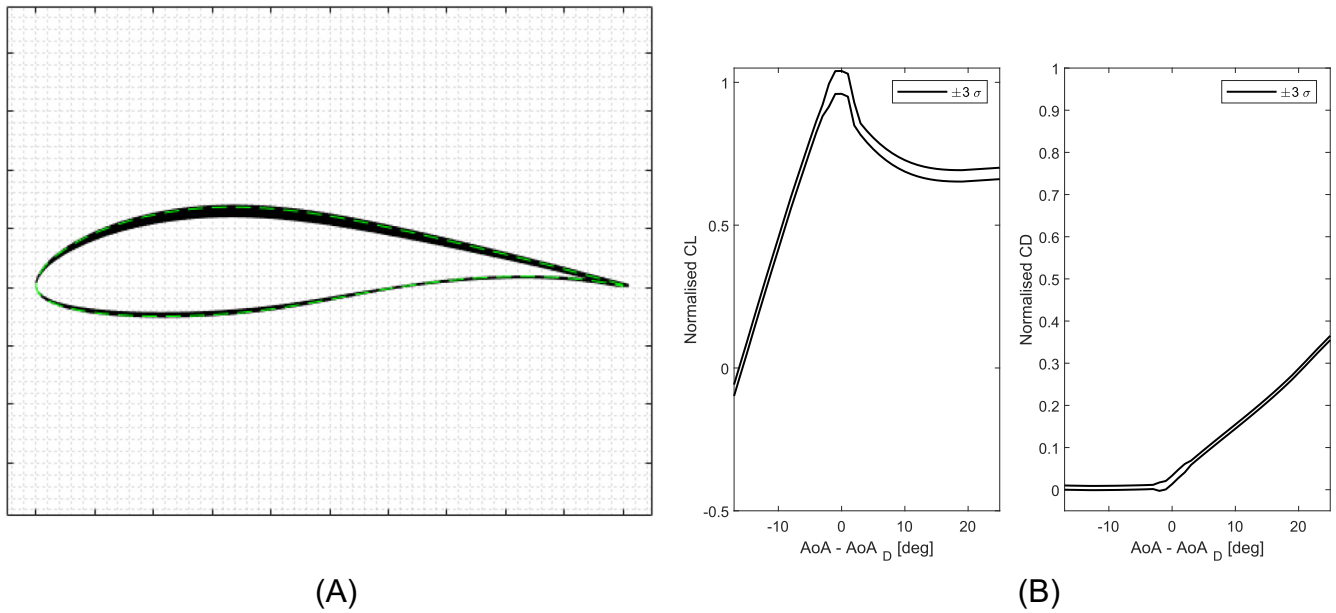


**FIGURE 6** (A) Aerofoil geometric tolerance and (B) confidence interval for lift and drag curves

**TABLE 5** Uncertainty in aerodynamic parameters

	CL (normal distribution)			CD (normal distribution)		
	Geometric Clean	Wind tunnel		Geometric Clean	Wind tunnel	
		Clean	Rough		Clean	Rough
High range	±3°	±3°	±5°	±3°	±3°	±5°
Region High (CoV)	4%	3%	3.5%	1%	1%	2%
Region Low (CoV)	2%	1%	1%	0.5%	0.5%	1%

of its nominal value (samples from this distribution can be seen in Figure 6A, where the green dashed line represents the nominal geometry). XFOIL<sup>22</sup> requires the simulation to be done over an aerofoil with unit chord length, so after a sample is generated, the new chord has to be normalised before it is simulated (which then gives the appearance of a thickness uncertainty seen in Figure 6).

The Monte Carlo simulation shows an impact of around 2% of the  $CL_D$  (design lift coefficient) in the linear region of the CL curve and an impact of around 4% of the  $CL_D$  in the region close to stall ±2% deg of the  $AoA_D$  (angle of attack for the design CL), Figure 6B. Table 5 summarises the results for both lift and drag coefficients.

### 3.2 | Wind tunnel measurements

There can be a range of factors contributing to the uncertainty in the measurement of aerofoil aerodynamic static coefficients in wind tunnels.<sup>23</sup> The focus herein will be on the results obtained when measuring the same aerofoil geometry ( $RT = 18\%$ ) in various wind-tunnels and two different surface conditions. Figure 7 shows 17 independent measurements in clean condition and 6 in rough conditions for the same aerofoil geometry. The black line is the nominal (clean aerofoil) values. The rough measurements were obtained by the use of ZigZag tape of different thickness, varying between 0.2 and 0.6 mm in regions between 2% and 5% of the chord on the suction side, and 5%–10% of the chord on the pressure side.

The scatter in the wind tunnel data can also be used to build a stochastic model for the clean and rough behaviour. In the same fashion as the geometric tolerances, the uncertainty model can be defined in two regions: one of *High* uncertainty, around the  $CL_D$  (or  $AoA_D$ ) and another of *Low* uncertainty defined as the remainder of the domain, illustrated by Figure 8. However, the regions cannot be defined in the same range for both clean and rough, as can be seen in Figure 7, the high uncertainty range in the rough behaviour is larger than on the clean. Table 5 shows the ranges of high uncertainty and the CoV in terms of the  $CL_D$ .

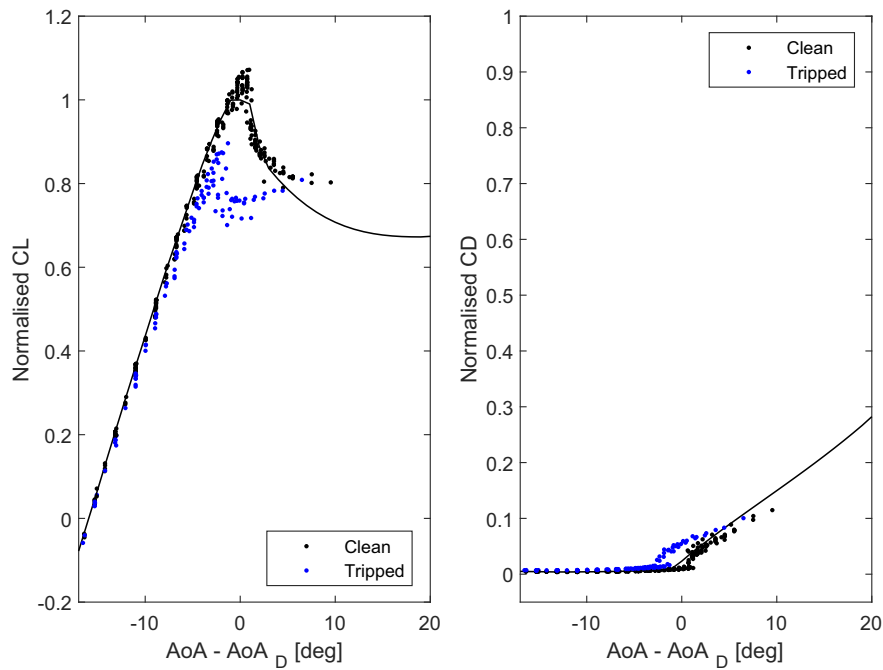


**FIGURE 7** Wind tunnel measurements: Clean and rough states

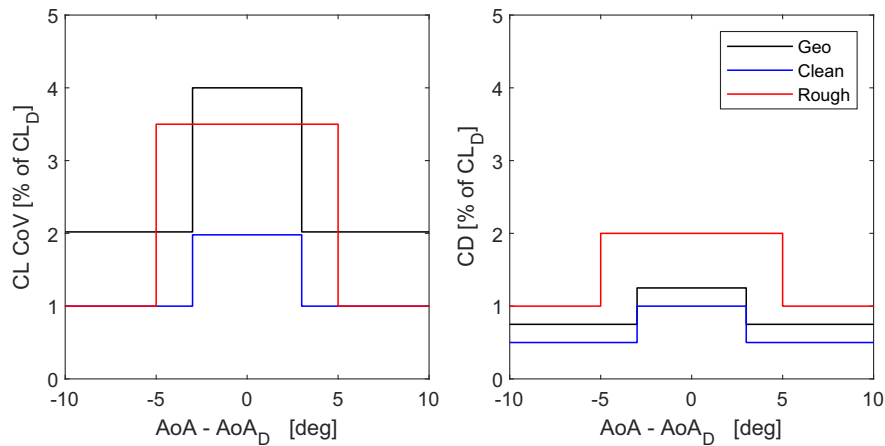


**FIGURE 8** CoVs for uncertainty in wind tunnel measurements: clean and rough

### 3.3 | Parametrisation of rough behaviour

In order to generalise the wind tunnel results, it becomes useful to have the rough behaviour characterised in terms of a parameter that can be (easily) identified in other aerofoils; one solution for that is to parametrise the rough CL and CD curves by the clean CL design value ( $CL_D$ ), and the angle of attack ( $AoA$ ) at which it happens ( $AoA_D$ ). This way one can describe the rough behaviour in terms of changes applied to the CL (and CD) curve.

Figure 9A shows the change in CD and CL in terms of the  $CL_D$ , as seen in the wind-tunnel tested aerofoil.

This model can be compared to the wind tunnel measurements, showing how close this parametrisation is to the experimental rough behaviour. Figure 9B shows the results of this parametrisation (the red line represents the mean value of the measurements for rough condition,

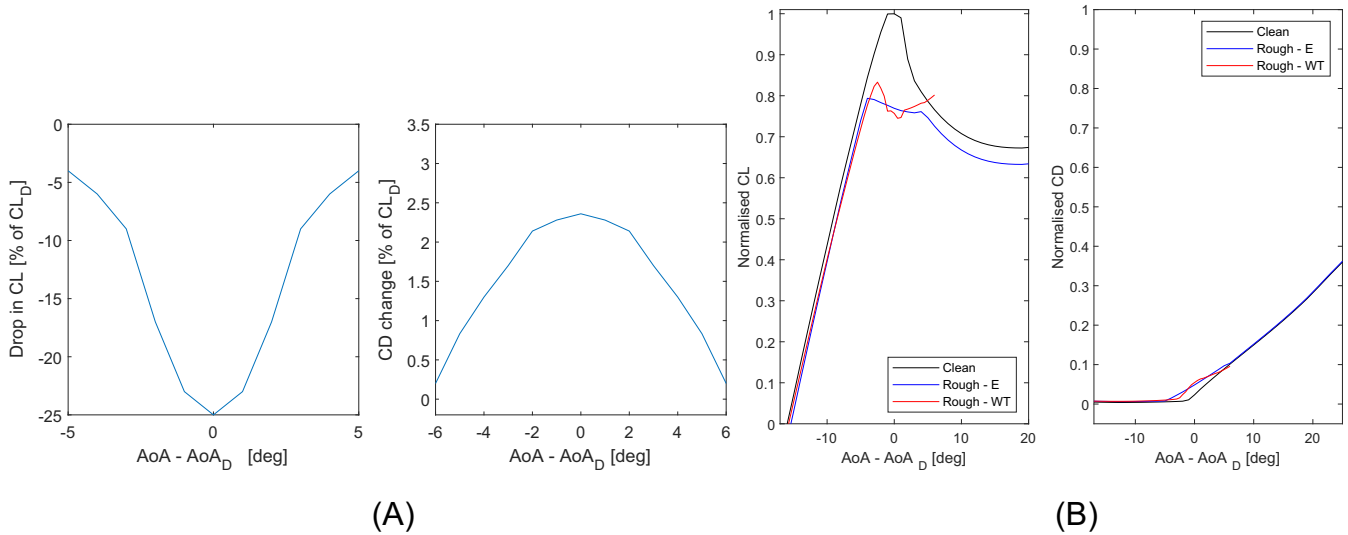


**FIGURE 9** Wind tunnel measurements: parametrisation (A) and validation (B) of the model

the blue line the rough behaviour parametrised in terms of the clean  $CL_D$ ). Even though this is not a perfect physics-based model, this parametrisation allows the approximation of a rough behaviour for aerofoils where only the clean characteristics are known.

### 3.4 | Extrapolation from wind tunnel measurements

Whereas the wind tunnel data shown in Figure 7 and the parametrisation shown in Figure 9 are particular to one of the aerofoils used in a blade, they can still be used to build an extrapolation to characterise the aerodynamic properties in rough condition of the whole blade. This approximation is necessary, because to characterise the actual rough behaviour for all of the blades' aerofoils would require an intangible number of experiments and that would be both impracticable and costly. Note that this approximation might introduce further uncertainties to the model but, as will be shown in Section 3.5, knowledge of the exact rough behaviour of the aerofoil is not necessary because the stochastic model developed in this study interpolates between clean and rough conditions, with only a limited contribution from the rough.

Because thick aerofoils (which are used close to the blade-root section) respond differently to surface roughness than slender aerofoils like the one shown in Figure 6 (normally used towards the tip of the blade), there is a need to define a separated characterisation for thick aerofoils 'rough conditions'. Even though the discussion of the aerodynamic phenomena causing this different behaviour is out of the scope for this study, it is important to find an appropriate description to this development, so that the developed model is closer to reality. To account for the lack of wind-tunnel measurements for thick aerofoils, an approximation to Van Rooji<sup>12</sup> results for the DU 00-W-401 is used for the aerofoils with RT (relative thickness) between 35% and 50%; a CL curve for this approximate rough behaviour can be seen in Figure 12A. For aerofoils with  $RT > 50\%$ , an interpolation between Van Rooji<sup>12</sup> results and the aerodynamic coefficients of a cylinder are used to define the rough behaviour.

### 3.5 | Stochastic model

To build a stochastic model of the aerodynamic coefficients of a wind turbine blade with the goal of building a pool of randomly-generated blades, there is a need to account for each of the uncertainty sources:

1. Uncertainty from geometric tolerances.
2. Uncertainty from wind-tunnel measurements (around the clean behaviour).
3. Uncertainty from wind-tunnel measurements (around the rough behaviour).
4. Uncertainty on aerodynamic degradation of the blade.

The first three uncertainties have been previously defined, the last source is addressed first by the model for degradation uncertainty and level of profile unevenness introduced by Bortolotti,<sup>10</sup> which defines a particular blade state as an interpolation between fully-clean and

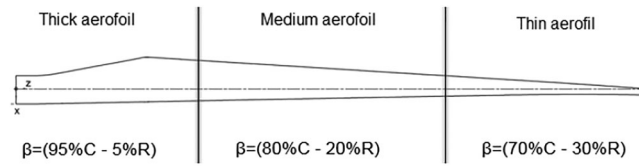


FIGURE 10 Blade regions

TABLE 6 Blade regions: Beta PDF definition

Location	Expected value [%]	Parameter	
		$a_1$	$a_2$
Root	5	4	75
Mid	20	2	8
Tip	30	5	11.66

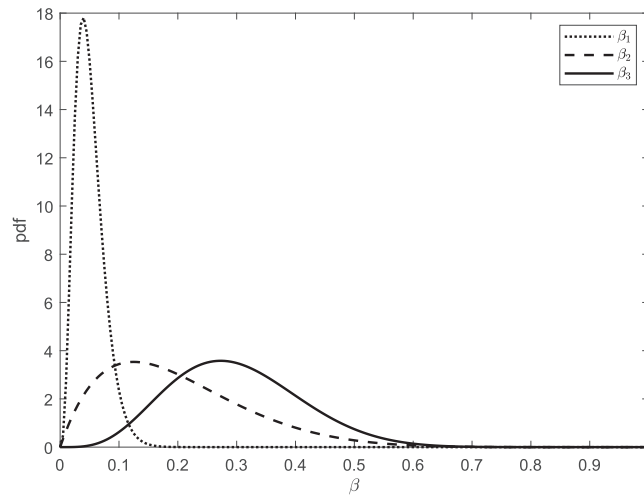


FIGURE 11 Betas PDFs for blade regions

fully-rough states by means of a variable  $\beta$ , following a beta distribution (Equation (3)), where 1 means a fully-rough and 0 a fully-clean aerofoil. The interpolation for a particular blade state is defined by

$$C_L = C_{LR} \cdot \beta + C_{LC} \cdot (1 - \beta) \quad (2)$$

In addition, the expected level of aerodynamic degradation can also vary through the blade span; aerofoils towards the tip are subject to higher speeds, which can make them more susceptible to erosion/degradation. In contrast, the root section experiences much lower velocities and therefore the expected degradation level is limited. This phenomenon motivates the introduction of a spatial variation in roughness levels throughout the blade. To include this progression in the stochastic model, the blade is divided into three sections as seen in Figure 10; The first section, closest to the blade root has an expected mean contribution of the rough aerofoil of 5%, the second and middle section of 20%, and the last, closest to the tip, of 30%. The parameters that define each beta distribution  $a_1$ ,  $a_2$  parameters are presented in Table 6 and shown in Figure 11, where

$$P(a_1, a_2) = \frac{x^{a_1-1} (1-x)^{a_2-1}}{B(a_1, a_2)}, \quad B(a_1, a_2) = \frac{\Gamma(a_1)\Gamma(a_2)}{\Gamma(a_1+a_2)} \quad (3)$$

where  $\Gamma$  is the Gamma function.

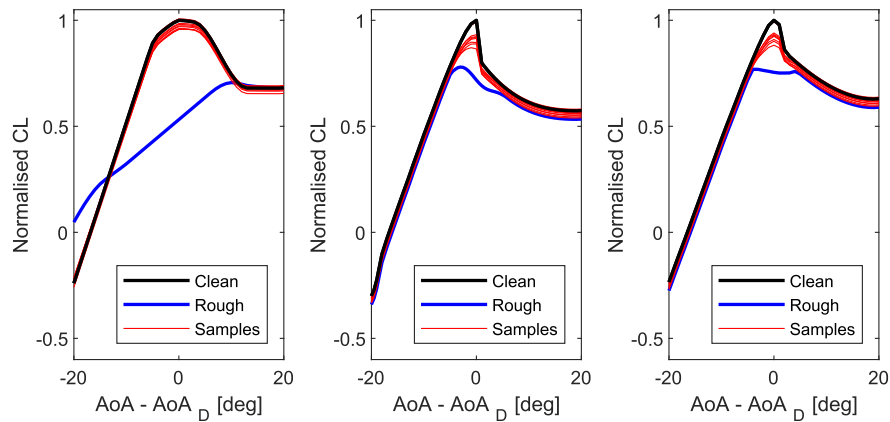


**FIGURE 12** CL for blade mixed aerofoil, respectively root, mid and tip

Figure 12 shows samples for CL curves on each of the three blade regions (root ( $RT = 50\%$ ), mid ( $RT = 35\%$ ), and tip ( $RT = 18\%$ )), where the respective expected contributions from the rough behaviour are 5%, 20% and 30% (Table 6). The procedure to generate a random mixed aerofoil characteristic can be defined as follows:

1. Account for the geometric uncertainty tolerance by sampling from a normal distribution with the specified CoV related to the range of AoA (defined in Table 5). The geometric uncertainties are applied for both clean and rough behaviour, CD and CL; they can be interpreted as a ‘perturbation’ to the nominal (clean and rough) behaviours.
2. Account for the uncertainty of the clean and rough behaviour (coming from the measurement uncertainty) on top of the geometric uncertainties by sampling from another normal distribution (Table 5). Here the samples for clean and rough are considered to be fully correlated (i.e. the aerofoil which would have the highest clean CL, will also have the highest rough CL).
3. Account for the uncertainty in spatial degradation of the blade by sampling from the beta distributions (defined in Table 6 and shown in Figure 11). All three beta distributions are fully correlated.
4. Use the  $\beta_i s$  to define the aerodynamic coefficients by interpolation (Equation (2)), for each aerofoil on the blade.

Figure 12 shows that the variation of randomly-generated samples from this stochastic model is closer to the clean state than to the rough. The parametrisation from wind-tunnel measurements (used on mid and thin aerofoils) and the approximation to Van Rooji<sup>12</sup> results (used on thick aerofoils) can be considered a good-enough approximation for the problem of defining rough-blade behaviour. In the next section, the effect of these uncertainties will be investigated in the turbine behaviour.

## 4 | AEROELASTIC TURBINE SIMULATION

### 4.1 | Uncertainty quantification for wind turbine loads

Aeroelasticity studies the interaction between the aerodynamic, inertial and elastic forces to which wind turbines are subjected. Aeroelastic simulations of wind turbines are an important tool to support the expansion of wind energy and provide the industry and the certifying institutions with models capable of performing complete simulations of the behaviour of wind turbines over a wide range of configurations and operational conditions.<sup>24</sup> A minimum set of these conditions is described in standards of wind turbine simulation in order to guarantee the safety and reliability of the design. To model and simulate wind turbines, several aeroelastic tools and methods are available, which include aerodynamic and structural components to determine loads and dynamic response of the structure.<sup>25</sup>

The analysis of this section was performed using the aeroelastic code BHawC,<sup>26</sup> to simulate a 5- to 10-MW pitch-controlled offshore turbine with a rotor diameter between 150 and 200 m in design load case (DLC) 1.2, according to IEC,<sup>5</sup> at three distinct wind speeds: cut in, rated and cut out. This DLC simulates the turbine subjected to atmospheric turbulence that occurs during normal operation of its lifetime. Class B<sup>5</sup> for medium turbulence characteristics was used in the setup.

The structural model in BHawC is built around the co-rotational formulation providing geometric nonlinearity.<sup>26</sup> The substructures for the tower, shaft and blades are modelled using Timoshenko beam elements which are defined by continuous cross-section properties tabulated in a reduced cross-section format.<sup>27</sup> The aerodynamic model is included via aerodynamic coefficient inputs related to each aerofoil of the blade span. Wind turbulence follows the IEC<sup>5</sup> standard, using the approach defined by Mann.<sup>28</sup>

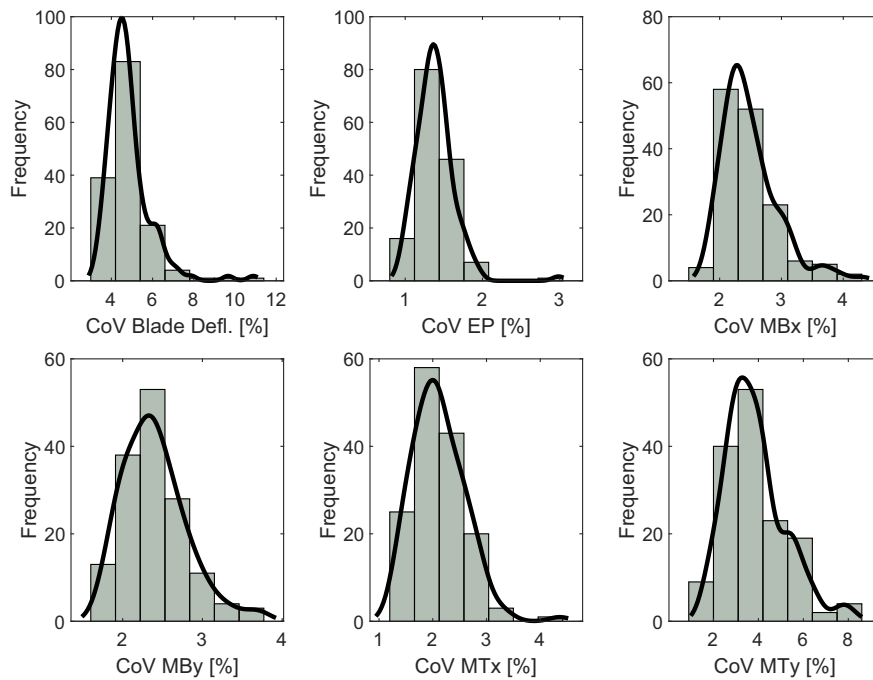


**FIGURE 13** Most likely CoV for rated wind speed

**TABLE 7** Loads CoV: ULS and FLS

Wind speed	Location	Cut in (%)		Rated (%)		Cut out (%)	
		ULS	FLS	ULS	FLS	ULS	FLS
Energy Production		3.5		1.8		1.3	
Blade Tip deflection	Tip	6.0		6.1		5.9	
Blade Flapwise moment	Root	6.0	8.9	3.0	7.4	5.7	4.8
Blade Edgewise moment	Root	3.4	2.5	3.0	2.3	5.6	3.0
Tower Fore-aft moment	Base	8.7	10.8	2.5	6.4	9.0	8.1
Tower Side-side moment	Base	9.0	7.1	6.7	6.6	10.4	11.7

From Sections 2 and 3, 150 samples are generated from the structural characterisation, 150 samples are generated from the aerodynamic characterisation and 150 seeds are generated from the turbulence model to define the wind profiles.

An LHS is used to define 5000 samples from the  $150 \times 150 \times 150$  possible combinations. These 5000 simulations are grouped with respect to the 150 wind seeds to find the most likely CoVs, as illustrated by Figure 13; the goal is to estimate the uncertainty caused on loads by structural and aerodynamic uncertainties without the effect of the seed variation. Both ultimate (ULS) and equivalent fatigue (FLS) loads are analysed.

The equivalent fatigue loads<sup>29</sup> are from

$$S_o = \left( \frac{\sum_i n_i S_i^m}{N_{eq}} \right)^{1/m} \quad (4)$$

where  $N_{eq}$  is the equivalent number of cycles to which one is calculating the equivalent load  $S_o$ ,  $m$  is the Wöhler slope;  $m = 10$  and  $m = 5$  for blade and tower loads respectively, and  $S_i$  is the load range which is determined based on Rainflow counting.

The normalised load CoVs, for both ultimate and fatigue equivalent loads are presented in Table 7. The CoVs related to the highest mean values are highlighted. General observations are as follows:

- For loads, the CoVs are calculated from the collection of maximum absolute values of the 5000 time series. For the energy production, the CoVs are calculated from the collection of mean values of the 5000 time series.

- The highest CoV is around 10% for the tower side-side moment at cut-out wind speed. This is the wind speed on which this load has its maximum mean value, thus is the channel where the uncertainties in blade structure and aerodynamic have the most significant impact.
- There is an overall trend of smaller impact of uncertainties at the rated wind speed (blade deflection, edge and flapwise moment, tower fore-aft moment), which might be explained by the fact that at this speed there is only limited pitching of the blade, thus operating with small variation in AoA and being subjected to less uncertainty of the aerodynamic coefficients.
- For tower loads, the fatigue-equivalent follows the same trend (of having the smaller CoV at rated) but for blade equivalent fatigue loads the behaviour is different: at flapwise the smallest CoV is at cut out.
- Overall fatigue-equivalent load CoVs are higher than ultimate-load CoVs, but these might be overestimated as they are averaged on 5000 simulations of 10min instead of the turbine lifetime and the Wöhler-weighting, as the variation in the ULSs loads go through the  $1/m$  exponent which will expectedly increase the CoVs for FLS.
- The blade-deflection CoV is the highest at rated wind speed; this is also where the highest deflection occurs, meaning that is also the wind speed where there could be a higher risk of blade-tower collision because of to excessive deflection.
- Tower loads have in general, higher CoVs than blade loads.

In Tarp-Johansen et al,<sup>30</sup> the uncertainty in the aerodynamics is modelled by a Gumbel distribution with a coefficient of variation of 10% for ultimate loads. Additionally, the model includes variation in material properties (5%), dynamic response (5%), exposure (10%-15%) and the annual maximum load (15%) which partly include the structural and turbulence uncertainty which is taken into account in this paper. The results indicate that the current stochastic models applied in the literature for, for example, calibration of partial safety factors for the IEC 61400-1 standard perhaps are too conservative for ultimate loading.

## 4.2 | Sensitivity analysis via regression coefficients

The primary objective of performing a sensitivity analysis is to assess the relative importance of the random inputs (aerodynamic or structural uncertainties) with relation to the output (turbine loads). There are several methodologies to study sensitivity, including meta-models, one-factor-at-a-time and variance-based methods.<sup>31</sup>

A particularly useful approach is based on linear regression of Monte Carlo simulations (also known as Standardised Regression Coefficients<sup>32,33</sup>). First, a linear model for each output needs to be obtained in terms of the inputs,

$$Y_i = m_0 + sX_1 + aX_2 + \dots + \varepsilon \quad (5)$$

where  $Y$  is the output,  $X_i$  the inputs,  $s$  the regression coefficients related to the structure,  $a$  to the aerodynamic and  $\varepsilon$  the residual that can be caused by interaction (I) between inputs, inadequacy of the linear model and turbulence uncertainty. These coefficients can be normalised by the ratio of the standard deviation of each input ( $\sigma_A$  = standard deviation of the  $CL_D$ ,  $\sigma_S$  = standard deviation of the mean flapwise stiffness) to the standard deviation of each load ( $\sigma_Y$ ),

$$S = s \frac{\sigma_{X_i}}{\sigma_Y}, \quad A = a \frac{\sigma_{X_i}}{\sigma_Y} \quad (6)$$

$S$  and  $A$  are defined as the sensitivity measure or the standardised regression coefficients.

In Section 2, the mean flapwise stiffness was defined as a parameter to represent the stochastic behaviour of the blade structure with relation to the uncertainties in the laminate parameters. This measure will be used in the sensitivity analysis, as there is a bigger interest in differentiating the contribution coming from structural and aerodynamic uncertainty sources instead of trying to define the relation between specific uncertainties in material properties to wind turbine loads.

In Section 3, the stochastic model of aerodynamic coefficients was defined parametrised in terms of a  $CL_D$ ; here, this parameter (which is specific to one aerofoil, but correlated to the whole blade because of the model) is used as the aerodynamic input to the sensitivity study.

The results of the variance decomposition are shown in Figure 14; they indicate how much each of the uncertainty sources contributes to the total variance of the chosen output that can be explained by the linear model: (A) aerodynamics, (S) structural and (I) interaction.

An interesting evolution of contribution for different wind speeds can be seen in the results that are coherent with aspects of the turbine operation (e.g., pitch control). The following conclusions can be made based on Figure 14, which shows the variance contribution for ULS.

- Overall, the linear model is best suited to distinguish between aerodynamic and structural uncertainties at rated wind speed. This can be explained by the operation point of the turbine; at rated wind speed there is limited pitching of the blades, meaning that they are operating

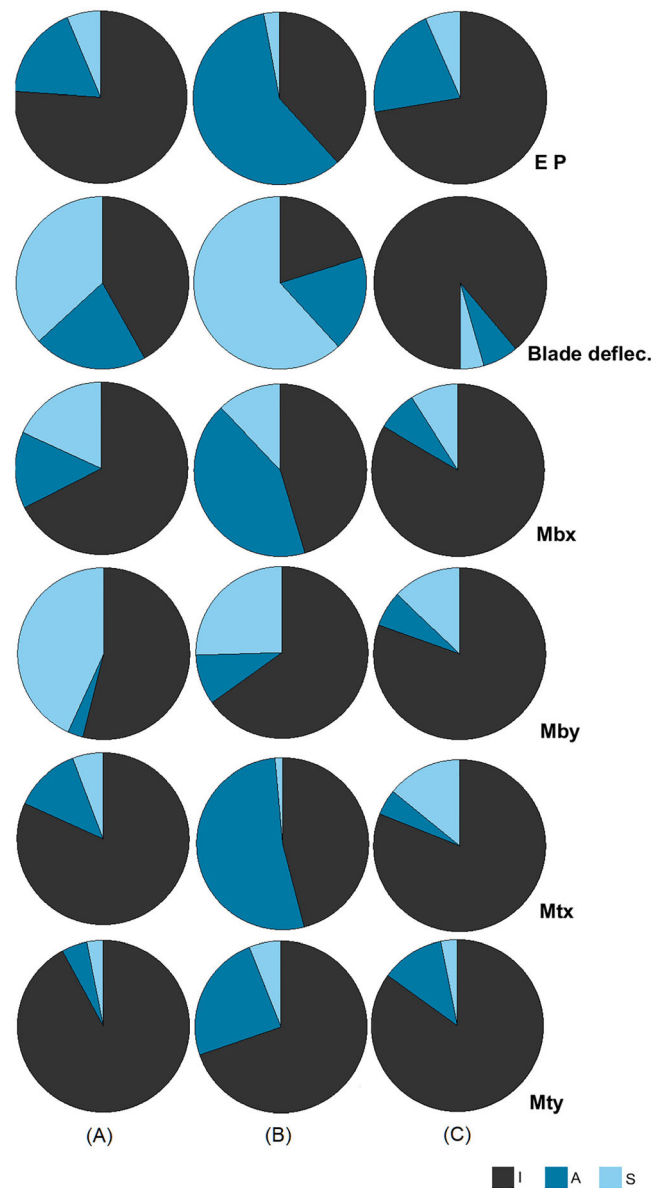


**FIGURE 14** Variance decomposition at (A) cut in (B) rated and (C) cut out wind speed

fully facing the wind, allowing them to capture as much energy as possible and that there are no other phenomena (e.g., turbine control actions) interacting.

- The variation in the aerodynamic coefficients is the main driver of energy production uncertainty; at all wind speeds it is the main contributor to the variance, with the highest contribution at rated. This observation is consistent with the importance given to having a good characterisation of these coefficients in wind turbine simulations.
- Blade deflection is highly influenced by the structural uncertainties, with over 60% of variance contribution at rated wind speeds. It is also interesting to note that, at cut out, because the blades are pitched out of the wind, the contribution from the structure is diminished.
- For both blade edgewise and tower side-side moment, most of the variance cannot be explained by a linear model, which means there is a higher level of interaction between the uncertainties and another methodology (nonlinear) should be used to study its sensitivity.

## 5 | CONCLUSION

This study demonstrated the characterisation of structural and aerodynamic uncertainties based on the variation of laminate properties and on wind tunnel measurements of aerodynamic coefficients. The propagation of these uncertainties to turbine loads was performed via a Monte Carlo simulation with a Latin hypercube sampling.



In Section 2, the effect of material property uncertainties on the blade structure was investigated. The laminate material properties were characterised by coupon testing, and their uncertainty propagated through the blade structural model. The stochastic characterisation (around 3% in mean flapwise stiffness, 0.5% in CG location and 1% in blade mass) was validated against blade static-deflection test and blade-weight measurements. Even though there might be other sources of uncertainty affecting the blade structure, this description is aligned with the behaviour observed in full-scale blade tests, motivating the propagation to the turbine level.

Another major uncertainty source was investigated in Section 3; the aerodynamic coefficients of the blade were described with the help of wind-tunnel measurements. The rough behaviour was extrapolated from one aerofoil to the complete set used in the blade by means of a parametrisation based on the maximum lift coefficient. The effects of geometric uncertainties were also characterised with respect to the tolerances defined by the standard.<sup>4</sup> A model for the spatial variation of surface roughness was defined and used to generate synthetic CL and CD curves for the aerofoils set. The model results in a range between  $-12\%$  and  $+4\%$  change of the CL max of a specific aerofoil (compared to nominal values), supporting the suitability of the extrapolation for the rough behaviour (as the aerodynamic coefficients simulated are much closer to the clean behaviour).

The CoVs for ultimate loads and fatigue equivalent loads were defined and the variance contribution investigated via standardised regression coefficients. The findings indicate that these uncertainties of blades have an effect on turbine loads of up to 10% (in ultimate tower side-side moment), and that for different loads at wind speeds, the variance contribution coming from structural or aerodynamic uncertainties is different. In general, tower loads in both directions were more affected than blade loads.

The variance contribution at cut-out wind speed is where there are the smallest linear effects captured by the SRC; this means that the interaction (and the turbulence) is responsible for most of the uncertainty levels in the loads. Rated wind speed results showed the best fitting of the SRC, with the linear phenomena explaining most of the variance.

These results also show the importance of a correct characterisation of the blade structure, to have a well-defined blade to tower clearance, as the IEC<sup>5</sup> specifies that blade-to-tower clearance (i.e., blade deflection) should be designed with a safety factor of at least 1.15. Whilst the effects of the aerodynamic and structural uncertainties have to be evaluated in other design load cases, at normal power production the uncertainty is only 6%, which brings the possibility of using uncertainty quantification to support the reduction of this safety factor. This study also shows that the standard approach can be challenged and improved upon as long as there are data. The good news is that wind turbine standards IEC 61400<sup>4</sup> require that tests are performed with both the composite material (coupons) used for the blades and the full-scale blade. Meaning that most likely, necessary data already exist in the production processes and can be taken into account in the design process, uncertainty quantification and reliability estimation, which would help the path to a cheaper and optimised blade design.

Stochastic modelling can become an important tool in the design of wind turbines. With the current trend of increased rotor sizes (and power ratings), optimisation has never been more important; thus, developing a full understanding of the effect that uncertainty can have on design critical parameters can be a part of the solution to decrease levelised cost of energy. Future research should integrate other uncertainty sources in the aeroelastic simulation as wind characterisation, damping estimation and expand the analysis to other design load cases.

## ACKNOWLEDGEMENTS

This project has received funding from the European Union's Horizon 2020 research and innovation programme under the Marie Skłodowska-Curie grant agreement No 764547.

## PEER REVIEW

The peer review history for this article is available at <https://publons.com/publon/10.1002/we.2715>.

## DATA AVAILABILITY STATEMENT

Research data are not shared. The data are not publicly available due to privacy (commercial) restrictions.

## ORCID

Paulo Gonzaga  <https://orcid.org/0000-0002-9970-5865>

## REFERENCES

1. Van den Bos L, Sanderse B. Uncertainty quantification for wind energy applications—literature review. CWI - Report SC-1701; 2017.
2. Bigoni D. Uncertainty quantification with applications to engineering problems. PhD Thesis: Technical University of Denmark; 2015.
3. Iec 61400-22:2010. Wind turbines—part 22: conformity testing and certification.
4. Iec 61400-5:2020. Wind turbines—part 5: wind turbine blades.
5. Iec 61400-1:2019. Wind turbines—part 1: design requirements.
6. Iec 61400-12-1:2017. Wind turbines—part 12: power performance.
7. Dimitrov NK, Lazarov BS. Reducing wind turbine load simulation uncertainties by means of a constrained gaussian turbulence fields. In: Proceedings of the 12th International Conference on Applications of Statistics and Probability in Civil Engineering (ICASP12); 2015.

8. Robertson A, Shaler K, Sethuraman L, Jonkman J. Sensitivity of uncertainty in wind characteristics and wind turbine properties on wind turbine extreme and fatigue loads. *Wind Energy Sci Discuss.* 2019;4:1-41. <https://doi.org/10.5194/wes-2019-2>
9. Papi F, Balduzzi F, Ferrara G, Bianchini A. Uncertainty quantification on the effects of rain-induced erosion on annual energy production and performance of a Multi-MW wind turbine. *Renew Energy.* 2021;165:701-715. <https://doi.org/10.1016/j.renene.2020.11.071>
10. Bortolotti P, Canet H, Bottasso C, Loganathan J. Performance of non-intrusive uncertainty quantification in the aeroservoelastic simulation of wind turbines. *Wind Energy Sci.* 2019;4(3):397-406. <https://doi.org/10.5194/wes-4-397-2019>
11. Abdel-Rahman A, Chakroun W. Surface roughness effects on flow over aerofoils. *Wind Eng.* 1997;21(3):125-137. <http://www.jstor.org/stable/43749639>
12. van Rooij RPJOM, Timmer WA. Roughness sensitivity considerations for thick rotor blade airfoils. *J Sol Energy Eng.* 2003;125(4):468-478. <https://doi.org/10.1115/1.1624614>
13. Abdallah I, Natarajan A, Sørensen JD. Impact of uncertainty in airfoil characteristics on wind turbine extreme loads. *Renew Energy.* 2015;75:283-300. <https://doi.org/10.1016/j.renene.2014.10.009>
14. Cappugi L, Castorriani A, Bonfiglioli A, Minisci E, Campobasso M. Machine learning-enabled prediction of wind turbine energy yield losses due to general blade leading edge erosion. *Energy Convers Manag.* 2021;245:114567. <https://doi.org/10.1016/j.enconman.2021.114567>
15. ISO 527-4:1997. Tensile properties of isotropic and orthotropic fiber-reinforced plastic composites—part 4: test conditions for isotropic and orthotropic fibre-reinforced plastic composites. International Organization for Standardization, Geneva, Switzerland.
16. Cover T, Thomas JA. Information theory and statistics. *Elements of Information Theory.* Vol. 1. New York: Wiley; 1991;279-335.
17. Krenk S, Jeppesen B. Finite elements for beam cross-sections of moderate wall thickness. *Comput Struct.* 1989;32:5.
18. Simms D, Schreck S, Hand M, Fingersh LJ. Nrel unsteady aerodynamics experiments in the nasa ames wind tunnel: a comparison of predictions to measurements. NREL/TP-500-29494. 2001. <https://doi.org/10.2172/783409>
19. Loeven G, Bijl H. Airfoil analysis with uncertain geometry using the probabilistic collocation method. In: *49th AIAA/ASME/ASCE/AHS/ASC Structures, Structural Dynamics, and Materials Conference*; 2008. <https://doi.org/10.2514/6.2008-2070>
20. Petrone G, de Nicola C, Quagliarella D, Witteveen J, Iaccarino G. Wind turbine performance analysis under uncertainty. In: *49th AIAA Aerospace Sciences Meeting including the New Horizons Forum and Aerospace Exposition*; 2011.
21. Rosemeier MMS. Impact of manufacture-induced blade shape distortion on turbine loads and energy yield. *J Phys: Conf Ser.* 2020;1618:52011.
22. Drela M. XFOIL: An analysis and design system for low reynolds number airfoils. In: Mueller TJ, ed. *Low Reynolds Number Aerodynamics. Lecture Notes in Engineering.* Vol. 54. Berlin, Heidelberg: Springer; 1989. [https://doi.org/10.1007/978-3-642-84010-4\\_1](https://doi.org/10.1007/978-3-642-84010-4_1)
23. Bak C, Madsen H, Gaunaa M, et al. Comparisons of airfoil characteristics for two airfoils tested in three different wind tunnels. In: *The DAN-AERO MW Experiments: Final report.* Denmark. Forskningscenter Risø. Risø-R, no. 1726(EN), Danmarks Tekniske Universitet, Risø Nationallaboratoriet for Bæredygtig Energi, Roskilde.
24. Ahlstrom A. Aeroelastic simulation of wind turbine dynamics. *PhD thesis:* Swedish Royal Institute of Technology - Department of Mechanics; 2005.
25. Ageze M, Hu Y, Wu H. Wind Turbine Aeroelastic Modeling: Basics and Cutting Edge Trends. *Int J Aerosp Eng.* 2017;2017:1-15. <https://doi.org/10.1155/2017/5263897>
26. Rubak R, Petersen J. Monopile as part of aeroelastic wind turbine simulation code. In: *In proceedings of copenhagen offshore wind denmark*; 2005; Copenhagen, Denmark.
27. Couturier P, Skjoldan P. Monopile as part of aeroelastic wind turbine simulation code. *J Phys: Confer Ser.* 2018;1037.
28. Mann J. Wind field simulation. *Probabilistic Eng Mech.* 1998;13(4):269-282. [https://doi.org/10.1016/S0266-8920\(97\)00036-2](https://doi.org/10.1016/S0266-8920(97)00036-2)
29. Thomsen K. The statistical variation of wind turbine fatigue loads. Riso national laboratory technical report Riso-R-1063(EN); 1997.
30. Tarp-Johansen N, Madsen P, Frandsen S. Partial safety factors for extreme loads effects. Riso national laboratory technical report Riso-R-1319(EN); 2002.
31. Helton J, Davis F. Latin hypercube sampling and the propagation of uncertainty in analyses of complex systems. *Reliab Eng Syst Saf.* 2003;81(1):23-69. [https://doi.org/10.1016/S0951-8320\(03\)00058-9](https://doi.org/10.1016/S0951-8320(03)00058-9)
32. Sin G, Gernaey KV, Lantz AE. Good modeling practice for pat applications: propagation of input uncertainty and sensitivity analysis. *Biotechnol Progr.* 2009;4:1043-1053.
33. Velarde J, Kramhøft C, Sørensen JD. Global sensitivity analysis of offshore wind turbine foundation fatigue loads. *Renew Energy.* 2019;140:177-189. <https://doi.org/10.1016/j.renene.2019.03.055>

**How to cite this article:** Gonzaga P, Toft H, Worden K, et al. Impact of blade structural and aerodynamic uncertainties on wind turbine loads. *Wind Energy.* 2022;1-17. doi:10.1002/we.2715